Faraday Discussions

Accepted Manuscript

This manuscript will be presented and discussed at a forthcoming Faraday Discussion meeting. All delegates can contribute to the discussion which will be included in the final volume.

Register now to attend! Full details of all upcoming meetings: http://rsc.li/fd-upcoming-meetings

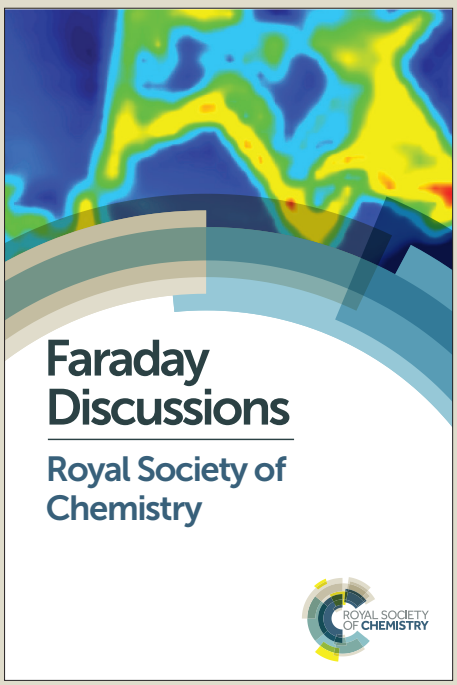

This is an *Accepted Manuscript*, which has been through the Royal Society of Chemistry peer review process and has been accepted for publication.

Accepted Manuscripts are published online shortly after acceptance, before technical editing, formatting and proof reading. Using this free service, authors can make their results available to the community, in citable form, before we publish the edited article. We will replace this *Accepted Manuscript* with the edited and formatted *Advance Article* as soon as it is available.

You can find more information about *Accepted Manuscripts* in the Information for Authors.

Please note that technical editing may introduce minor changes to the text and/or graphics, which may alter content. The journal's standard Terms & Conditions and the Ethical guidelines still apply. In no event shall the Royal Society of Chemistry be held responsible for any errors or omissions in this *Accepted Manuscript* or any consequences arising from the use of any information it contains.

ROYAL SOCIETY OF CHEMISTRY

www.rsc.org/faraday_d

Probing the Excited State Relaxation Dynamics of Pyrimidine Nucleosides in Chloroform Solution

Katharina Röttger[1,2], Hugo J. B. Marroux[1], Hendrik Böhnke[2], David T.J. Morris[1], Angus T. Voice[1], Friedrich Temps[2], Gareth M. Roberts[1]* and Andrew J. Orr-Ewing[1]*

[1]*School of Chemistry, University of Bristol, Cantock's Close, Bristol, BS8 1TS, UK*
[2]*Institut für Physikalische Chemie, Christian-Albrechts-Universität zu Kiel, Olshausenstr. 40, D-24098 Kiel, Germany*

*Correspondence to: a.orr-ewing@bristol.ac.uk; g.m.roberts@bristol.ac.uk

Abstract

Ultrafast transient electronic and vibrational absorption spectroscopy (TEAS and TVAS) of 2'-deoxy-cytidine (dC) and 2'-deoxy-thymidine (dT) dissolved in chloroform examines their excited-state dynamics and the recovery of ground electronic state molecules following absorption of ultraviolet light. The chloroform serves as a weakly interacting solvent, allowing comparisons to be drawn with prior experimental studies of the photo-dynamics of these nucleosides in the gas phase and in polar solvents such as water. The pyrimidine base nucleosides have some propensity to dimerize in aprotic solvents, but the monomer photochemistry can be clearly resolved and is the focus of this study. UV absorption at a wavelength of 260 nm excites a $^1\pi\pi^* \leftarrow S_0$ transition, but prompt crossing of a significant fraction (50% in dC, 17% in dT) of the $^1\pi\pi^*$ population into a nearby $^1n\pi^*$ state is too fast for the experiments to resolve. The remaining flux on the $^1\pi\pi^*$ state leaves the vertical Franck-Condon region and encounters a conical intersection with the ground electronic state of ethylenic twist character. In dC, the $^1\pi\pi^*$ state decays to the ground state with a time constant of 1.1 ± 0.1 ps. The lifetime of the $^1n\pi^*$ state is much longer in the canonical forms of both molecules: recovery of the ground state population from these states occurs with time constants of 18.6 ± 1.1 ps in amino-oxo dC and ~114 ps in dT, indicating potential energy barriers to the $^1n\pi^*/S_0$ conical intersections. The small fraction of the imino-oxo tautomer of dC present in solution has a longer-lived $^1n\pi^*$ state with a lifetime for ground state recovery of 193 ± 55 ps. No evidence is found for photo-induced tautomerization of amino-oxo dC to the imino-oxo form, or for population of low lying triplet states of this nucleoside. In contrast, ~8% of the UV-excited dT molecules access the long-lived T_1 ($^3\pi\pi^*$) state through the $^1n\pi^*$ state. The primary influence of the solvent appears to be the degree to which it destabilizes the states of $^1n\pi^*$ character, with consequences for the lifetimes of these states as well as the triplet state yields.

Faraday Discussions Accepted Manuscript

1. Introduction

The photochemistry of the four canonical DNA nucleobases has undergone intense study within the chemical physics community,[1, 2] largely through a drive to better understand their avoidance of photochemical damage following the absorption of solar ultraviolet (UV) radiation (i.e., their photostability). The advent of ultrafast spectroscopy[3] and advances in theoretical methods for treating electronically excited states[4] have revealed that this photostability is a direct consequence of the ultrashort lifetimes of optically bright electronically excited $^1\pi\pi^*$ states,[1] brought about by (often barrierless) access to an array of conical intersections between the ground (S_0) and excited states.[5, 6] However, even with their intrinsic resistance to UV-induced degradation, photodamage can still occur when the nucleobases are embedded within double- or single-stranded DNA. Unlike the purine derived bases (adenine and guanine), the pyrimidine bases, cytosine and thymine (Fig. 1, R = H), are particularly susceptible to mutagenic photodimerization pathways, such as (2+2) cycloaddition and (6-4) adduct formation, which must then undergo energetically costly enzymatic photorepair.[7-9] Various schools of thought have emerged to rationalize the susceptibility of pyrimidines to photo-reactions, which invoke both the trapping of excited population in reactive triplet states[10-12] and, more generally, the role of dynamic conformational fluctuations in the DNA duplex.[13] In this work, we specifically revisit the photochemistry of the pyrimidine nucleosides (Fig. 1). We examine the ultrafast photodynamics of chloroform solutions, and compare with prior studies in water, acetonitrile and methanol to explore what impact (if any) this more weakly interacting solvent environment has on the excited state relaxation dynamics of the pyrimidine nucleosides. Chloroform also provides a dielectric medium for the nucleobases similar to that experienced within the core of a DNA double helix.[14]

The relaxation dynamics of the cytidine nucleoside (C) have been studied in various solution phase environments[15-21] as well as in isolated species in the gas phase.[22] Following excitation to the bright $^1\pi\pi^*$ state at wavelengths from 260 – 270 nm in aqueous solution, a range of transient absorption methods reveal that excited state population decays bi-exponentially with time constants of 720 fs and ~30 ps.[15-18, 21] Similar dynamics have also been found for C in chloroform through ultrafast fluorescence up-conversion.[19] Numerous theoretical studies[23-35] on the relaxation

Faraday Discussions Accepted Manuscript

pathways available to the simpler cytosine nucleobase do not yield a single unified picture of the dynamics, returning (at least) three calculated conical intersections with their relative importance to excited state deactivation depending on the level of theoretical treatment, particularly in dynamics simulations.[31, 36-38] However, experimentalists have broadly elected to ascribe the sub-picosecond time constant to direct relaxation to S_0, most likely *via* an 'ethylenic-twist' type $^1\pi\pi^*/S_0$ conical intersection, while the slower 30 ps component has been associated with the decay of population trapped in a $^1n\pi^*$ state, formed following initial ultrafast $^1\pi\pi^* \rightarrow {}^1n\pi^*$ bifurcation in the vertical Franck-Condon (vFC) region.[17] This slower $^1n\pi^*$ channel was only revealed through bleach recovery kinetics[17, 18] and transient absorption decay at $\lambda \leq 340$ nm,[17] indicating that this state is optically dark to excited state absorption (ESA) in the visible wavelength region.[16, 17] Most importantly though, the lifetime of the $^1n\pi^*$ decay channel shows a clear dependence on both the chemical substituent (R) present in the N1 position (Fig. 1) and the solvent environment; in aqueous cytosine (R = H) it is reduced to 12 ps (*cf.* ~30 ps in aqueous C).[17, 18, 21] This substituent effect is also found in the gas phase,[39] although the exact origins of this behaviour are not yet fully understood.

Ultrafast spectroscopy studies on the thymidine nucleoside (T) at wavelengths spanning 260 – 270 nm return a qualitatively similar picture to the relaxation dynamics observed for C;[11, 15-17, 20, 22, 40-43] in aqueous solution, bi-exponential decay of the excited state population to S_0 occurs *via* the bright $^1\pi\pi^*$ (540 fs) and dark $^1n\pi^*$ (127 ps) states.[15-17] A host of theoretical calculations[28, 37, 44-52] on the isolated thymine nucleobase led experimentalists to propose the above interpretation for the extracted time constants. However, transient vibrational absorption spectroscopy (TVAS) measurements by Kohler and co-workers on T in acetonitrile-d_3 indicate a significant fraction of excited state flux also undergoes intersystem crossing (ISC) into a long-lived T_1 ($^3\pi\pi^*$) triplet state (with lifetime $\tau \approx 0.6$ μs).[11] Note that although the quantum yield for ISC is $\phi_{ISC} \approx 0.2$ for dT in acetonitrile-d_3, ISC is an order of magnitude less probable for aqueous T ($\phi_{ISC} \leq 0.02$).[53] In agreement with theory,[46, 51] these authors suggested that ISC most likely occurs from the dark $^1n\pi^*$ surface, rather than $^1\pi\pi^*$, although they were only able to determine a lower-limit of ≤10 ps for $^1n\pi^* \rightarrow {}^3\pi\pi^*$ transfer. To the best of our knowledge, no analogous TVAS experiments

Faraday Discussions Accepted Manuscript

have studied triplet state formation in C, although, in principle, ISC may be possible, given a small but measurable phosphorescence quantum yield for C,[54] and bleach recovery kinetics suggesting $\phi_{ISC} \leq 0.07$ in water.[17]

In this discussion paper, we report the use of ultrafast optical spectroscopy, in both the UV/visible and mid-infrared (IR) spectral regions, supported by spectral assignments based on density functional theory (DFT) calculations, to probe the excited state relaxation dynamics of chemically modified cytidine and thymidine 2'-deoxy-nucleosides (dC and dT, with d denoting the 2'-deoxyribose form). All experiments are performed on low concentrations (≤50 mM) of silyl-protected 2'-deoxy-nucleosides in chloroform. For dC, the excited state relaxation dynamics, following excitation at 260 nm, are tracked using both transient electronic (UV/visible) absorption spectroscopy (TEAS) and TVAS. Unlike in water, dC in chloroform at 298 K is present in two different tautomers: the canonical amino-oxo (AO) and minor imino-oxo (IO) forms (see Fig. 1). Although both tautomers display bi-phasic excited state relaxation dynamics, the $^1n\pi^*$ channel is ~9 times slower in the IO form, relative to AO. In the case of dT, only TVAS is used to probe the relaxation dynamics. Unlike dC, we see the presence of only a single dT tautomer and clear evidence for triplet state formation on a picosecond timescale with a quantum yield of $\phi_{ISC} \approx 0.08$. Triplet state decay for dT in chloroform occurs over more than 1 ns. Although triplet states are discussed to be the precursor for thymidine dimerization in solution,[55-60] we do not see evidence for the diffusion-limited formation of dT dimers within 1.3 ns. Minor contributions from hydrogen-bonded dC•dC and dT•dT homodimers are also observed in both cases, although a detailed analysis of their dynamics will remain the subject of a future study.

2. Methods

2.1 Synthesis

To enable sufficient solubility of dC and dT in aprotic solvents, such as chloroform, the ribose OH groups of the 2'-deoxy-nucleosides were protected by bulky, apolar *tert*-butyldimethylsilyl (TBDMS) groups (see Fig. 1). The synthesis in Kiel followed

Faraday Discussions Accepted Manuscript

a modified protocol of Ogilvie.[61] The synthesis for protected dC and dT at the University of Bristol was described in detail in a recent publication.[62]

2.2 Transient Electronic Absorption Spectroscopy

TEAS experiments were performed at the University of Kiel, and the details of the apparatus have been presented elsewhere.[63, 64] The transient absorption experiment was driven by the output of a Ti:Sapphire laser (ClarkMXR CPA 2001) which delivers pulses with pulse lengths of 150 fs (FWHM) at 775 nm. Half of the overall output of 1000 μJ/pulse was used for the transient absorption experiment. The excitation pulses were generated in a non-collinear optical parametric amplifier (NOPA) with subsequent temporal compression and frequency doubling. The resulting pulses had a centre wavelength of 260 nm and a bandwidth of ~ 4 nm. For the generation of the broadband probe pulses, ~70 μJ/pulse of the laser fundamental was used. The laser pulses passed a delay stage (M-531.DG, Physik Instrumente) equipped with a retroreflector (CVI Melles Griot). They were attenuated to ~ 2 μJ by an absorptive neutral density filter and a combination of a λ/2 waveplate and a polarizer. These pulses were focused into a CaF_2 plate (d = 2 mm, Korth Kristalle) to produce a white-light continuum. The CaF_2 plate was rastered vertically and horizontally so that consecutive laser pulses hit different spots, thus ensuring that the low damage threshold of CaF_2 was not exceeded. The white light pulses were split into probe and reference beams using the front and back reflections from a planar glass plate. Pump and probe pulses were recollimated using reflective optics to reduce the chirp and obtain an optimal time resolution of the experiment. The pump pulses were set to magic angle polarization with respect to the probe pulses using a λ/2 waveplate. An optical chopper (MC2000, Thorlabs) equipped with a 10 shot blade (MC1F10, Thorlabs) was used to cut out every second laser pulse, thus enabling the measurement of background signals without excitation. The transmitted broadband light pulses were dispersed in a prism spectrograph and detected by two full-frame transfer back-thinned CCD cameras (Entwicklungsbüro Stresing, Berlin).

The sample solutions were circulated through a home-built flow cell equipped with two quartz windows (d = 0.2 mm, diameter 15 mm, Korth Kristalle) and a PTFE

Faraday Discussions Accepted Manuscript

spacer of 100 μm thickness. A gear pump (Reglo-Z analog, Ismatec) equipped with an organic solvent resistant pumphead (Z-186 with PPS gears, Ismatech) and PTFE tubes was employed to flow the sample solution continuously through the cell. Transient absorption measurements for each sample and the neat solvent were measured in one experimental run to avoid a change of coherent solvent signals. The cross-correlation of pump and probe pulses and the instrument response function were both ~50 fs. Each sample and solvent measurement was repeated three times to ensure reproducibility, and all measurements were repeated at least two times on different days with fresh sample solution. The purity and integrity of the samples were checked before and after each measurement via UV/vis absorption spectroscopy. The water content was reduced by preparing all sample solutions with anhydrous $CHCl_3$ in a flow box purged with dry air and checked before and after the transient absorption measurements via IR spectroscopy. For the TEAS experiments, 2',3',5'-*tri*-O-(*t*-butyldimethylsilyl)-cytidine (C) was used instead of the protected 2'-deoxy-nucleoside (dC). As was shown previously,[65] the dynamics are virtually the same for the protected C and dC molecules. All TEAS measurements were performed with sample concentrations of c_0 = 10 mM.

2.3 Transient Vibrational Absorption Spectroscopy

TVAS experiments were performed at the University of Bristol, using an apparatus that has been described in detail previously.[66] Briefly, the system consists of a Coherent Vitara-S oscillator and Coherent Legend Elite HE+ regenerative amplifier, operating at 1 kHz and configured to produce 40 fs duration pulses at 800 nm with a total output power of 5 W. This fundamental beam was split into three parts using a series of beam splitters. Only two of these beams were used for the current measurements, each with an energy of 2.45 mJ/pulse. The two beams seeded two Coherent OPerA Solo optical parametric amplifiers (OPAs). One of these OPAs produced spectrally tunable light spanning the UV to IR range (220 – 20,000 nm) and was used to generate the 260 nm (~100 fs) pump pulses for all the TVAS experiments reported here. The remaining OPA generated broadband (~300 cm^{-1}) tunable IR pulses for use as a probe in TVAS experiments, with energies of ~1 μJ/pulse at the sample.

Faraday Discussions Accepted Manuscript

For the TVAS measurements on dC and dT, the 260 nm pump pulse was attenuated to between ~0.6 and 1 μJ/pulse by cross-polarization using a λ/2 waveplate and wire-grid polarizer, and then focused ~2 cm behind the sample by a f = 250 mm CaF_2 lens. A beam profiler was used to determine a ~250 μm beam diameter for the Gaussian profile (full-width at half maximum) of the pump beam at the sample, returning pump fluences in the range 1.2 – 2 mJ cm^{-2}. The polarization of the UV pump was maintained at the magic angle (54.7°), relative to the polarization of the IR probe pulse, by using the λ/2 waveplate in the UV pump beam line.

Broadband IR probe pulses were generated by difference frequency generation of the signal and idler beams from the IR OPA. In the experiments described here, the IR light was centred at ~1680 cm^{-1} (carbonyl stretching region) or ~3400 cm^{-1} (N-H stretching region). The entire IR probe beam line was enclosed by sealed plastic tubes and continuously purged by dry N_2 to avoid undesired absorption by atmospheric water vapour and CO_2. The IR probe pulses were reflectively focused into the sample to a tight ~50 μm beam diameter, so that the probed region of the sample was uniformly excited by the more loosely focused UV pump beam. The cross correlation of pump and probe pulses was 120 fs, but the instrument response function was longer (200-400 fs) because of thermal lensing effects.

The temporal delay (t) between the UV pump and IR probe pulses was controlled by changing the path length of the pump beam with an aluminium retro-reflector mounted on a motorized delay stage, providing a maximum possible delay of t = 1.3 ns. The pump and probe beams then intersected the sample with a small crossing angle of ~5°. Prior to interaction with the sample, the UV pump beam was modulated at 500 Hz (blocking every other pulse) with an optical chopper wheel to obtain pump on/off spectral pairs at each t, which were then used to generate individual transient absorption spectra. After passing through the sample, the transmitted IR probe light was detected by a 128 pixel, liquid N_2 cooled Mercury Cadmium Telluride array (Infrared Associates Inc., MCT-10-128) coupled to a spectrometer (HORIBA Scientific, iHR320), providing a spectral resolution of ~2 cm^{-1}.

Faraday Discussions Accepted Manuscript

Sample solutions of protected dC (c_0 = 5 mM) and dT (c_0 = 50 mM) were prepared in anhydrous $CDCl_3$ or $CHCl_3$ (Sigma-Aldrich, 99.99%). These sample solutions were then delivered through a stainless steel flow cell, containing two 1.5 mm thick CaF_2 windows separated by either a 200 or 380 μm thick Teflon spacer, which defined the absorption path length. The sample solution was flowed continuously through the cell by a peristaltic pump with PTFE tubing throughout.

3. Results and Discussion

Time-resolved vibrational and electronic absorption spectroscopies provide information on both the UV-photoexcited states of dC and dT and their relaxation pathways back to the ground state. We first present TEAS and TVAS measurements for dC solutions in chloroform and then TVAS results obtained for the corresponding dT solutions. The amino-oxo (AO) and the minor imino-oxo (IO) tautomeric structures adopted by the monomeric dC nucleosides in chloroform are shown in Fig. 1, together with the single structure for monomeric dT. Possible hydrogen-bonded dT•dT dimer structures are also shown. In the gas phase, the cytosine nucleobase also adopts an enol tautomer of the AO form,[67] but connection of a ribose group to the N1 atom in the ring to form the nucleoside removes this possibility in our solutions. The minority IO tautomer of dC has two conformers distinguished by the *trans* or *cis* arrangement of the imino group. It can be identified by a characteristic IR absorption band at 1725 cm^{-1} in chloroform solution.[62, 68] Computational studies of the photochemistry of cytosine and its 1-methyl derivative identified conical intersections between the $^1\pi\pi^*$ (S_1) and S_0 states, passage through which leads to bifurcation on the ground S_0 state to produce both the AO and IO tautomers.[32, 33] These computations therefore suggest a photochemical route for AO to IO conversion, as observed in argon matrix studies of 1-methylcytosine.[69]

The propensity for the silyl-derivatized nucleosides to dimerize in aprotic solvents can be quantified by a solvent-dependent equilibrium constant, and in the case of dC in chloroform the association constant K_{CC} = [dC•dC]/[dC]^2 = 42.8 ± 2.1 M^{-1} was previously determined by Schwalb *et al*.[19] The degree of association is given by the parameter β_{CC} = 2[dC•dC]/c_0, where c_0 = [dC] + 2[dC•dC] is the prepared

Faraday Discussions Accepted Manuscript

concentration of the dC solution. The degree of association and the fractions of dC and dC•dC can be evaluated from c_0 using the known value of K_{CC}. We also note that this previous study by Schwalb *et al*. identified only a single symmetric dC•dC dimer structure in chloroform (see Fig. 1 in Ref. 19). We undertook a similar analysis of concentration dependent steady state FTIR spectra of dT in chloroform solutions, examples of which are shown in panels (a) and (b) of Fig. 2, to evaluate the corresponding association constant K_{TT} and degree of association β_{TT} for dT solutions (Fig. 2(c)). The analysis used spectra obtained in the N-H stretching region (Fig. 2(b), 3100 – 3450 cm^{-1}); in the carbonyl stretching region (Fig. 2(a), 1600 – 1800 cm^{-1}), the monomer and dimer bands in the corresponding spectra overlap too much to be analysed. We obtained K_{TT} = 2.1 ± 0.7 M^{-1}, which indicates a lower propensity to dimerize than dC. Table 1 summarizes the degrees of association for different solutions with c_0 values in the range used in our current study. Fig. 1 shows three possible isomers of the dT•dT dimer, and our FTIR spectra in the carbonyl stretching region suggest dimer 1 is the form most commonly adopted in chloroform. Comparison of the measured FTIR spectra for 10 mM and 50 mM solutions of dT (Fig. 2(a)) reveals a dimer contribution at the low wavenumber side of the carbonyl stretching band of the monomer. Predicted IR spectra for all possible dimer structures (with R = CH_3, Fig. 1) were obtained using Gaussian 09 [70] calculations at the B3LYP/6-311++G** level of theory, including a polarizable continuum model (PCM) for the chloroform solvent, and confirm that dimer 1 is the only candidate that shows a similar band shift to lower wavenumber.

We concentrate on TVAS data obtained in the carbonyl and N-H stretching regions of the nucleosides, but also considered the possibility that UV photoexcitation might cleave bonds in the heterocyclic rings, as seen in related systems.[68, 71] Homolytic ring-opening photochemistry should produce photoproducts with characteristically strong isocyanate bands around 2100 – 2200 cm^{-1}.[68] While no such features were observed for dT, TVAS measurements in this spectral region for dC revealed very weak (μΔOD changes in optical density) bands that might be assigned to isocyanate species. However, comparisons with band intensities in the carbonyl region under comparable conditions, demonstrates that the ring-opening pathways make negligible contributions to the pyrimidine nucleoside photochemistry.

Faraday Discussions Accepted Manuscript

3.1 Transient Spectroscopy of dC Solutions in Chloroform

The absorption of UV light of wavelengths around 260 nm by amino-oxo dC monomers dissolved in chloroform excites a $\pi^* \leftarrow \pi$ electronic transition. In the cytosine nucleobase, the resulting $^1\pi\pi^*$ state corresponds to the S_1 state in the vFC region[30] (albeit with $^1n\pi^*$ states close in energy, and lower than the $^1\pi\pi^*$ state at some levels of theory[6, 38]) and can undergo a number of possible fates. These include direct internal conversion to the ground S_0 electronic state *via* an ethylenic-twist type conical intersection, internal conversion to the nearby $^1n\pi^*$ state (S_2 in the vFC region), or perhaps ISC to the T_2 ($^3n\pi^*/^3\pi\pi^*$) or T_1 ($^3\pi\pi^*$) triplet states.[6] The $S_1 \rightarrow T_1$ conversion is forbidden by the El Sayed rules[72] and ISC has therefore been proposed to occur following internal conversion to the $^1n\pi^*$ state,[17] or *via* $S_1 \rightarrow T_2$ conversion.[26, 34, 35]

Fig. 3(a) shows examples of TEA spectra obtained following 260-nm excitation of a 10 mM C solution in $CHCl_3$. At this concentration, approximately 65% of the C in solution is present as monomers and the remainder is dimers. The time-dependent TEA spectra are displayed as a 2D map, with colours indicating the intensities of transient features. These features are weak, but two components dominate the spectra: a broad, positive band at visible wavelengths is attributed to excited state absorption (ESA), while a negative feature in the near-UV corresponds to stimulated emission from the excited state. Neither band shows significant wavelength shifts over time. Decay of the majority of the signal intensity in both bands within a few picoseconds is consistent with the short excited state lifetimes measured previously for cytidine samples in other solvents or the gas phase.[15-17, 19-22]

The TEA spectra were analysed by selecting time-dependent intensity profiles at 8 wavelengths in the range 340 – 600 nm, two examples of which are shown in panels (b) and (c) of Fig. 3 for probe wavelengths of 340 nm and 560 nm, and simultaneously fitting to exponential decays. Three time constants emerge from these fits: $\tau_1 = 0.6 \pm 0.5$ ps for the decay of the stimulated emission signal, and $\tau_2 = 1.1 \pm 0.1$ ps and $\tau_3 = 193 \pm 55$ ps for the decay of the ESA. The large relative uncertainty

Faraday Discussions Accepted Manuscript

in the value of τ_1 is a consequence of the overlapping stimulated emission and ESA signals at early times. Because the three time constants are deduced from only a single sample concentration, we cannot decompose them further into contributions from C monomers and C•C dimers. Depopulation of the vFC region on the excited state potential energy surface accounts for the loss of the stimulated emission signal, and is commensurate with the shortest timescale reported in fluorescence up-conversion experiments.[19] The τ_2 value would appear to reflect the lifetime of molecules in the $^1\pi\pi^*$ state. It is therefore tempting to assign τ_3 to molecules that transfer from the $^1\pi\pi^*$ to the $^1n\pi^*$ state, but fluorescence up-conversion measurements suggested a lifetime of 21 ± 2 ps for the $^1n\pi^*$ state population,[19] which is hard to reconcile with the longer lifetime ESA component reported here. We return to this point below after consideration of the information obtained from TVAS.

TVA spectra in the carbonyl and N-H stretching regions provide further detailed insights, and example spectra are displayed in panels (a) and (d) of Fig. 4, respectively. These spectra were obtained using 5 mM solutions of dC in $CDCl_3$, for which we expect 76% dC monomers and 24% dC•dC dimers. In panels 4(a) and (d), negative changes in optical density (ΔOD) correspond to depletion of the ground state molecules by the UV laser pulse. We refer to these as ground state bleach features. Positive ΔOD values indicate intermediate or product species. The dominant bleach feature centred close to 1650 cm^{-1} in Fig. 4(a) has two overlapping components assigned to a carbonyl stretch (νCO) and a scissoring motion of the NH_2 group (νscis). A further weak bleach to lower wavenumber is attributed to a ring-stretching mode (νrs). The assignment of all these features to the AO tautomer of dC is supported by observation of corresponding absorption bands in the steady state FTIR spectrum.[19, 62] The weak bleach feature at 1725 cm^{-1} was previously assigned to a νCO mode of the IO tautomer of dC.[62, 68] Positive going features to the low wavenumber side of the bleaches are characteristic of absorptions by vibrationally hot, but electronically S_0 molecules formed by internal conversion from higher lying electronically excited states. These features grow and then decay over time as the excess vibrational energy of the molecules dissipates into the surrounding solvent.

Faraday Discussions Accepted Manuscript

In the N-H stretching region shown in Fig. 4(d), the two main bleach features are assigned to the symmetric (νNH_2s) and antisymmetric (νNH_2a) stretches of the NH_2 group of dC.[19] Again, signatures of vibrationally hot S_0 state molecules can be seen as transient absorption features to the low wavenumber sides of the bleaches. In both IR regions, the bleach features reduce in depth over time, and return to the baseline absorbance level. The absence of significant residual bleaches at times approaching the upper limit of 1.3 ns for our measurements demonstrates almost complete recovery of ground state dC molecules following absorption of 260-nm UV light, and we conclude that there is negligible formation of photoproducts (including long-lived triplet states). A suggestion of a small remaining depletion of the νCO mode at 1660 cm^{-1} and the νscis mode at 1645 cm^{-1} cannot be indicative of photoproduct formation because it is only observed for this pair of overlapping bands; instead, we attribute this residual bleach to an overlapping band of dC•dC dimers (see below).

Panels (b), (c), (e) and (f) of Fig. 4 show the time dependences of selected bleach and transient absorption features in the TVA spectra. These time-dependent intensities were obtained by integrating the band intensities over 10 cm^{-1} wide intervals about the band centres. Fits of the time-dependent band intensities to bi- or tri-exponential functions give the time constants (τ_n) and relative amplitudes (A_n) of each exponential component reported in Table 2. The recoveries of the bleaches of the carbonyl stretching band of the AO tautomer (νCO, 1660 cm^{-1}, panel (b)) and the NH_2 symmetric stretching band (νNH_2s, 3410 cm^{-1}, panel (e)) show similar time dependences. The same fast initial decays in amplitude are also seen in the carbonyl band bleach corresponding to the IO tautomer (νCO, 1720 cm^{-1}, panel (c)) and the transient absorption in the NH_2 symmetric stretching region by vibrationally hot S_0 molecules (ν^*NH_2, 3380 cm^{-1}, panel (f)). We therefore globally fitted all these kinetic decays to the same set of exponential functions to obtain a single set of time constants representing all the band intensity changes.

The recoveries of the bleach features of the AO tautomer are well-described by biexponential functions with the two components having similar amplitudes, and time constants of $\tau_4 = 6.2 \pm 0.3$ and $\tau_5 = 18.6 \pm 1.1$ ps. The combination of these two decays returns the bleach depths to within a few percent of their initial values. The

Faraday Discussions Accepted Manuscript

majority of the decay of the ν^*NH_2 feature at 3380 cm^{-1} also occurs with a 6.2 ± 0.3 ps time constant, indicating that this timescale corresponds to vibrational cooling of hot S_0 molecules formed by rapid internal conversion from the $^1\pi\pi^*$ (S_1) state. The prompt rise of the ν^*NH_2 feature confirms that this internal conversion is comparable to, or faster than, our experimental time resolution of 0.5 ps for TVA, consistent with the 1.1 ps lifetime of the $^1\pi\pi^*$ state deduced from our TEA spectra. As the molecules vibrationally cool, the ground electronic and vibrational level populations are recovered and the transient bleach of this ground state steadily disappears. The 6.2 ± 0.3 ps value is likely to be indicative of the timescales for the last few steps down the ladder of vibrational levels, or perhaps just the final cooling step from $v = 1 \rightarrow v = 0$ of a particular mode, which are expected to be rate determining.[66, 71] The same time constant describes the initial vibrational cooling of the IO tautomer, suggesting similar coupling of the internal modes of both tautomers to the solvent bath. We also observed similar time constants for vibrational cooling in our recent study of G•C Watson-Crick base pair photochemistry in chloroform.[62]

A significant component of the intensity (~50%) decays with a time constant of 18.6 ± 1.1 ps demonstrating a second, slower pathway to repopulation of the S_0 state. This lifetime agrees with the 21 ± 2 ps time constant reported from fluorescence up-conversion studies of dC in chloroform solution.[19] The evidence from electronic structure calculations and prior experimental studies of dC photochemistry points to the $^1n\pi^*$ state as an intermediate in this relaxation pathway. The 18.6 ± 1.1 ps time constant mostly reflects the lifetime of this state, because after the $^1n\pi^* \rightarrow S_0$ internal conversion, the vibrationally hot S_0 molecules will relax with the aforementioned 6.2 ± 0.3 ps time constant. The population of the $^1n\pi^*$ state is seen indirectly in our measurements through recovery of the ground state bleach, but not directly by TEAS. Previous studies of dC in water concluded that the $^1n\pi^*$ state is optically dark to further absorption in the near-UV and visible regions.[16, 17] Observation of this state by fluorescence up-conversion at wavelengths around 340 nm indicates a non-zero transition dipole moment to S_0,[19, 21] yet we do not see persistence of a stimulated emission feature over this timescale in our TEA spectra. Likely reasons are that the transition dipole moment to S_0 is weaker than for the $^1\pi\pi^* \rightarrow S_0$ emission, and not

Faraday Discussions Accepted Manuscript

detected at our low ΔOD levels, and that the emission lies at the short-wavelength edge of our TEAS detection window.

A residual offset of 3% of the maximum amplitude is seen for the bleach feature of the AO tautomer νCO band, and in the IO tautomer the corresponding residual offset is ~5%. This offset persists for the duration of our experiments (up to 1.3 ns) and is therefore described in Table 2 as an exponential decay component with 'infinite' time constant (τ_6). The most plausible explanation for this feature is UV photo-depletion of dC•dC dimers in the chloroform solution, with recovery of an equilibrium concentration of the dimers taking much longer than 1 ns. This assignment is supported by calculations of vibrational frequencies of the dimer which indicate bands in the 1625 - 1650 cm^{-1} region, and by concentration-dependent FTIR spectra of the dC solutions in chloroform. We discount formation of a long-lived triplet state of dC because the TVA spectra obtained in the N-H stretching region above 3300 cm^{-1}, which exclusively feature monomer bands (the broad hydrogen-bonded dC•dC dimer bands are observed below 3300 cm^{-1}, *cf.* Fig. 2(b)),[19] show complete recovery of the ground state population. The νNH_2s and νNH_2a bands of the T_1 state of the AO form of dC are calculated to shift by ~50 cm^{-1} to higher wavenumber from the ground state bleaches, and we do not observe product bands at the corresponding locations in our TVA spectra. The fast $S_1 \rightarrow T_2$ ISC with ~13% branching predicted by Richter *et al.*[34] in dynamical calculations for isolated AO cytosine is therefore not apparent in our study of the corresponding nucleoside in chloroform.

The bleach feature assigned to the IO tautomer (νCO at 1720 cm^{-1}) does not show a decay component with 18.6 ± 1.1 ps time constant. Instead, a much slower component with $\tau_3' = 162 \pm 48$ ps accounts for ~17% of the recovery of this bleach (Fig. 4(c)). The timescale for this decay appears to agree with the $\tau_3 = 193 \pm 55$ ps process observed in TEAS experiments. The likely explanation for this slower component is again diversion of some of the ensemble of relaxing molecules into the $^1n\pi^*$ state, but in the case of the IO tautomer this fraction is significantly smaller than for the AO tautomer, and the $^1n\pi^*$ state lifetime is almost an order of magnitude longer. The extended lifetime suggests that access to the conical intersection connecting the IO $^1n\pi^*$ state to the S_0 state is more restricted, perhaps lying at higher energy above the

Faraday Discussions Accepted Manuscript

minimum of the $^1n\pi^*$ state than is the case for the AO tautomer.[27] Unlike the case of the AO tautomer, the $^1n\pi^*$ state of the IO tautomer does not appear to be optically dark to ESA in the visible region. The fraction of IO is small in dC samples in chloroform, so the $^1n\pi^*$ state emission was not resolved from AO tautomer signals in fluorescence up-conversion experiments.[19]

A slow component fitted by the 162 ± 48 ps time constant also contributes ~12% of the amplitude of the relaxation of the ν^*NH_2 feature at 3380 cm^{-1} (Fig. 4(f)). This observation is consistent with an overlapping contribution to this spectral feature from the IO tautomer, with slow relaxation from the longer lived IO $^1n\pi^*$ state feeding into the later time intensity changes of this transient band.

We see no evidence for growth of the IO band corresponding to the previously proposed bifurcation of flux at the $^1\pi\pi^*/S_0$ conical intersection in theoretical calculations;[32, 33, 69] instead, the weak νCO bleach of the IO tautomer band returns to the baseline because of (nearly) complete ground state recovery of the initially photo-excited IO molecules. Nor do we observe any significant long-time bleaching of the ground state bands of the AO tautomers that might indicate photochemical conversion to the IO form, or to triplet states of the AO form of dC.

The various deductions from our TEAS and TVAS measurements of the AO and IO tautomers of dC in chloroform solution are summarized in Fig. 5. This figure shows schematic potential energy cuts along coordinates corresponding to the relaxation of the initially photo-excited molecules on the $^1\pi\pi^*$ state and *via* the $^1n\pi^*$ state. In the latter case, we consider distinct $^1n\pi^*$ potential energy landscapes for the AO and IO tautomers. Excitation in the vFC region by UV photon absorption draws its transition strength from the $^1\pi\pi^* \leftarrow S_0$ electronic character, but bifurcation along the two competing pathways in almost equal measure (for the AO tautomer) suggests strong coupling between the S_1 ($^1\pi\pi^*$) and S_2 ($^1n\pi^*$) states in the vFC region. The vFC region depopulates in ~0.6 ps, with subsequent relaxation on the $^1\pi\pi^*$ state accessing a conical intersection with the S_0 state. The total lifetime of the $^1\pi\pi^*$ state is ~1.1 ps under our experimental conditions. These timescales are controlled by the gradient of the path from the vFC region to the $^1\pi\pi^*/S_0$ conical intersection and a small barrier to

Faraday Discussions Accepted Manuscript

this conical intersection from the minimum of the $^1\pi\pi^*$ state.[6] Passage through the conical intersection returns flux to the S_0 state where vibrational cooling occurs with a 6.2 ps time constant. Approximately half the photo-excited AO tautomers instead branch into the $^1n\pi^*$ state where they are trapped with excited state lifetimes of ~18 ps before returning to the S_0 state through (or in the vicinity of) a conical intersection, and vibrationally cooling with a characteristic 6.2 ps time constant. The relaxation pathway on the $^1\pi\pi^*$ state is also observed in the IO tautomer, and is now the dominant (~80%) route back to the ground state. The remaining ~20% of photo-excited IO tautomers cross onto the $^1n\pi^*$ state where they remain with lifetimes of 162 ps before reaching the $^1n\pi^*/S_0$ conical intersection. Fig. 5 includes approximate molecular structures at the conical intersections, which are based on calculations for cytosine in the gas phase.[27, 37, 38]

The character of the $^1n\pi^*$ states merits some further consideration because the unpaired electron remaining in a non-bonding orbital might reside preferentially on an O or an N atom (denoted $^1n_O\pi^*$ or $^1n_N\pi^*$, respectively). Most prior computational and experimental studies of the excited states of the AO tautomer consider the $^1n\pi^*$ state to involve the non-bonding orbital on the carbonyl group (hence $^1n_O\pi^*$).[1, 6, 17] We have adopted this assignment in Fig. 5, but note that Quinn *et al*. presented arguments favouring a state involving excitation of an electron from the N-atom lone pair ($^1n_N\pi^*$).[18] They reported a band at 1574 cm^{-1} seen for aqueous solutions of dC and 2'-deoxy-cytidine 5'-monophosphate (dCMP) nucleotide, but not for cytosine, which they assigned to a vibration of the $^1n_N\pi^*$ state. This spectral feature indicated an excited state lifetime of 37 ps. We do not observe a band in our spectra of dC in chloroform that clearly corresponds to this feature in aqueous solutions, but different solvent interactions may simply have shifted it out of our observation window.

For the IO tautomer, calculations by Marian and co-workers indicated that the populated $^1n\pi^*$ state involves the non-bonding orbital of the N atom in the imine group.[27] On this basis, we propose that the energetic stabilization at the adiabatic minimum of this $^1n_N\pi^*$ state derives from the electron-deficient n_N-orbital of the imine mixing with the heterocyclic ring π-system when the imine group is rotated 90° out-of-plane (see the inset IO $^1n_N\pi^*$ minimum energy structure in Fig. 5).

Faraday Discussions Accepted Manuscript

3.2 Transient Spectroscopy of dT Solutions in Chloroform

The smaller association constant for dT than dC in chloroform means that the time resolved spectra presented here for dT solutions are dominated by monomer photochemistry. Comparisons of TVA spectra obtained for dT concentrations of 10 mM and 50 mM (4% and 15% association to dT•dT dimers, Table 1) show no differences, confirming negligible contribution from dT•dT dimers (or dynamics of the dimer that are indistinguishable from those of the monomer).

Fig. 6 displays TVA spectra of dT solutions in chloroform in the carbonyl (Fig. 6(a)) and N-H (Fig. 6(d)) stretching regions. These spectra were analysed by fitting to sets of Gaussian functions to obtain time-dependent band intensities. The fits were conducted using Origin 9.0. In the carbonyl stretching region, separate Gaussian functions described the νCO bleach (requiring 3 Gaussian functions with tied amplitudes), two hot ν*CO bands centred at 1657 and 1689 cm^{-1} and a νCO_{T1} product band (attributed to the T_1 ($^3\pi\pi^*$) triplet state – see below) centred at 1629 cm^{-1}. In the N-H stretching region, single Gaussian functions were used to fit the νNH bleach (3400 cm^{-1}), a ν*NH vibrational hot band (3380 cm^{-1}) and a νNH_{T1} product feature (3412 cm^{-1}). The plots in Figs. 6(b) and 6(d) show the time-dependences of the bands in these two spectral regions. As with the analysis of dC, the time-dependent band intensities are once again fitted to bi- or tri-exponential functions, returning the τ_n and A_n values collated in Table 3. The νCO bleach feature recovers ~80% of its amplitude with an exponential time constant of $\tau_1 = 5.3 \pm 0.6$ ps, with two slower components with ill-determined time constants estimated to be $\tau_2 \approx 114$ ps and $\tau_3 > 1$ ns (referred to as infinity within our experimental time window) accounting for the remaining recovery. When the νCO bleach recovery is fitted with the corresponding signals in the N-H stretching region, the average value obtained for the fastest resolved component of the S_0 recovery is $\tau_1 = 7 \pm 2$ ps, and this value is reported in Table 3. Approximately 8% of the initial νCO bleach amplitude remains at a time delay of 1 ns. Comparable observations are made for the νNH bleach recovery. The ν*CO vibrational hot band rises with a time constants of $\tau_4 = 2.4 \pm 0.6$ ps, most likely indicative of initial $v > 1 \rightarrow v = 1$ cooling in S_0. Both hot bands subsequently decay

Faraday Discussions Accepted Manuscript

with τ_1 = 5.3 ± 0.6 ps, a value that agrees with the dominant bleach recovery rate, likely determined by the final v =1 → v = 0 vibrational relaxation step in S_0.

Photoproduct bands are observed in both spectral regions and show growth that is delayed by τ_5 = 5-10 ps. Overlap of the product bands with bleach and hot band features prevents a more precise determination of the delay, but the product grows thereafter with a time constant of 5.3 ± 0.6 ps (νCO_{T1}) or 7 – 14 ps (νNH_{T1}). We highlight that the νNH_{T1} feature is heavily overlapped with the νNH bleach, so the deduced delay is less reliable than that extracted from νCO_{T1} analysis. In the carbonyl stretching region, the νCO_{T1} product band at 1629 cm^{-1} shows no decay within the 1.1 ns range of our experiment, consistent with the long-lived bleach feature. The positions of the product bands match expectations for the first excited T_1 ($^3\pi\pi^*$) triplet state from our calculated vibrational frequencies at the PCM-B3LYP/6-311++G** level of theory on the simpler 1-methylthymine (Fig. 1, R = CH_3) (Figs. 6(c) and (f)). This assignment accords with a previous report of thymine and dT photochemistry in acetonitrile-d_3, in which bands at 1603 and ~1700 cm^{-1} were assigned to the T_1 ($^3\pi\pi^*$) state.[11] This prior study observed complete growth of the T_1 ($^3\pi\pi^*$) triplet state population within 10 ps of UV photoexcitation. Kohler and co-workers also examined the photochemistry of thymine and thymidine 5'-monophosphate (dTMP) in aqueous solution by TEAS,[17] and deduced bifurcation of the excited state flux between ultrafast relaxation on the $^1\pi\pi^*$ state (accessing a conical intersection with the S_0 state), and slower picosecond relaxation *via* the $^1n\pi^*$ state. These deductions are broadly supported by subsequent calculations of excited state pathways and dynamics in the thymine nucleobase and various derivatives using a variety of theoretical methods, although the precise outcomes differ between calculations.[6, 44, 45, 47, 48, 50, 52] The $^1n\pi^*$ state lifetimes were deduced to be 30 ± 13 ps and 127 ± 15 ps for thymine and dTMP, respectively, in aqueous solution.[17]

Fig. 7 summarizes the photochemical pathways we observe, together with relevant calculated structures on the simpler thymine nucleobase.[37, 46] Guided by the earlier work on thymine and its derivatives, we assign the rapid rise of the vibrational hot bands of the S_0 state of dT in chloroform to ultrafast $^1\pi\pi^* \rightarrow S_0$ internal conversion *via* a conical intersection between these two electronic states (most likely involving

Faraday Discussions Accepted Manuscript

an ethylenic-twist), and the ~114 ps time constant to recovery of the S_0 ground state *via* the longer-lived $^1n\pi^*$ state. Our measurements suggest ~17% of the excited state flux undergoes $^1\pi\pi^* \rightarrow {}^1n\pi^*$ internal conversion around the vFC region. The > 1 ns persistence of the ground state bleaches is indicative of long-lived population in the T_1 ($^3\pi\pi^*$) state, formed with a quantum yield of $\phi_{ISC} \approx 0.08$.

The T_1 ($^3\pi\pi^*$) state of dT is unlikely to form directly from the photoexcited $^1\pi\pi^*$ state, both on orbital symmetry grounds[72] and because the lifetime of the UV populated $^1\pi\pi^*$ state is so short.[6, 49] Instead, it will be populated from the $^1n\pi^*$ state. Hare *et al*. previously argued that this $^1n\pi^* \rightarrow {}^3\pi\pi^*$ ISC process must occur before vibrational relaxation to the minimum of the $^1n\pi^*$ state to account for their TVAS observations in acetonitrile-d_3 solution.[11, 17] Our results in chloroform solution are not so clear-cut because the bands assigned to the T_1 state show an apparently delayed onset of 5-10 ps, whereas the T_1 state population growth was complete on this timescale according to the measurements in acetonitrile-d_3. Nevertheless, the picosecond time frame on which we observe evolution of the T_1 bands in chloroform is consistent with population *via* the longer lived $^1n\pi^*$ state and not the initially excited $^1\pi\pi^*$ state, and the timescale for growth of the T_1 band intensities is comparable with our expectations for vibrational cooling (*cf*. τ_5 vs τ_1, see Table 3). This cooling may occur in the $^1n\pi^*$ state or the $^3\pi\pi^*$ state, or both. Two candidates for the delayed onset of the triplet bands are plausible: (i) ISC occurs only after the $^1n\pi^*$ state has vibrationally cooled sufficiently to access the region of ISC, which must lie above the minimum of the $^1n\pi^*$ state otherwise population would continue to feed into T_1 over the ~114 ps lifetime of the excited $^1n\pi^*$ state; (ii) $^1n\pi^* \rightarrow {}^3\pi\pi^*$ ISC is prompt, but our TVAS measurements fail to observe molecules in the initially hot $^3\pi\pi^*$ state until they have relaxed to low vibrational levels. We observe one weak band at around 1600 cm^{-1} which appears to form promptly, and might be a signature of hot triplet state molecules, but its time dependence cannot be isolated in spectral fits. Similar difficulties in resolving absorption by vibrationally excited product molecules arose in our previous TVAS study of G•C Watson-Crick base pairs in chloroform.[62] Possible causes include spectral overlap (*e.g*. with strong ground state bleaches) and anharmonic spreading of the hot band intensities.

Faraday Discussions Accepted Manuscript

3.3 Solvent Effects on the Photodynamics of Cytosine and Thymine Derivatives

The nuclear dynamics that follow UV excitation to the vFC region of the $^1\pi\pi^*$ states of pyrimidine bases, and their nucleoside and nucleotides, are governed by the energetic proximity of $^1n\pi^*$ states and downhill pathways to conical intersections with the ground electronic state. In the case of thymine and its derivatives, interaction with the low lying triplet states is also significant. The relative energies of the $^1\pi\pi^*$ and $^1n\pi^*$ states, and their triplet counterparts, will be sensitive to the properties of the surrounding medium, as will the locations of conical intersections. The dielectric constant of the medium is a measure of electrostatic interactions, but the molecularity of a solvent, and the ultrafast dynamics of solvent-solute couplings may also play a role. Table 4 draws together the time constants and ISC quantum yields (ϕ_{ISC}) reported in previous and the current ultrafast laser studies for the various photochemical pathways of the pyrimidine bases and their derivatives in different solvents.

The gas-phase spectroscopy studies of Leutwyler and co-workers demonstrate that low-lying vibrational levels of the S_1 ($^1\pi\pi^*$) state of the AO form of cytosine, accessed at wavelengths of ~310 nm, have lifetimes of tens of picoseconds,[73] with the S_1 v = 0 level surviving for 730 ps.[39] Ultrafast fluorescence up-conversion measurements at 296 nm did not show this behaviour for the related dC nucleoside in chloroform solution.[19] When cytosine is excited to higher energies, using wavelengths below 290 nm, the low barrier from the zero-point level (v = 0) of the S_1 state to the conical intersection with the S_0 state does not substantially slow the internal conversion to the ground state; in both the gas-phase[67, 73-75] and several solvents,[21, 76-79] $^1\pi\pi^* \rightarrow S_0$ timescales of <2 ps are reported for cytosine and its derivatives. Similar behaviour is also observed for the C nucleoside in the gas-phase.[22] Some simulations of the non-adiabatic dynamics of isolated UV-excited cytosine suggest a much faster (<100 fs) contribution to the S_0 recovery that is not resolved in the solution-phase experiments.[31, 38] These ultrafast dynamics might be captured in the gas-phase time-resolved photoionization measurements on cytosine by Ullrich *et al.*[80] and Kosma *et al.*,[67] but the latter study ascribed them to wavepacket motion out of the vFC region, more consistent with the simulations of Hudock & Martinez[36] and Lan *et al.*,[37] with

Faraday Discussions Accepted Manuscript

internal conversion to S_0 on the 1.1 ps timescale. The 0.69 ps lifetime observed in the non-adiabatic dynamics calculations of Barbatti *et al.* was instead attributed to decay of the $^1n_O\pi^*$ state, but the 1.2 ps limit of the simulations precluded consideration of processes occurring over longer timescales.[38] Conversely, Hudock & Martinez[36] suggested that population on the $^1n_O\pi^*$ state is trapped for >1 ps, in-line with experimental interpretations.

Estimated triplet state yields for cytosine are at most a few percent, either in the gas-phase[39, 81] or aqueous solution.[17] Our measurements suggest that for the nucleoside in chloroform, triplet state formation is also negligible. The most significant effect of the choice of solvent appears to be on the lifetimes of the $^1n\pi^*$ states,[21] which are also sensitive to whether cytosine has a ribose group/chemical derivative attached at the N1 site.[17, 18, 39] In the case of the 2'-deoxy-ribose nucleoside, the $^1n\pi^*$ state lifetime is reduced in chloroform when compared with water and methanol,[18, 21] an effect that we consider unlikely to be caused by the peripheral TBDMS protecting groups present in our nucleoside derivative. The polar, protic solvents are expected to destabilize the $^1n\pi^*$ state with respect to the conical intersection with the S_0 state to a greater degree than chloroform does, which should extend the $^1n\pi^*$ lifetime. Alternatively, protic solvents might promote excited state isomerization to the imino-oxo tautomer which has a longer lived $^1n\pi$ state; the extended $^1n\pi^*$ lifetime is particularly noticeable in methanol solution,[21] with a lifetime similar to the minor IO form $^1n_N\pi^*$ state in chloroform reported here. Both values are also similar to the $^1n\pi^*$ lifetime deduced from gas-phase studies on IO cytosine.[67]

More generally, the forgoing discussion goes some way to highlighting that, despite extensive research, a unified picture has not been reached for the relaxation dynamics of cytosine and its derivatives, as recently acknowledged in a review by Improta *et al.*[6] The outcomes of computational studies depend sensitively on the chosen electronic structure calculation method, reflecting the importance of energy orderings of close lying excited states, energy gradients and the locations of conical intersections. The lack of consensus aptly demonstrates that the task of completely disentangling DNA photodynamics (even in the simpler nucleobases) is still a complex undertaking.

Faraday Discussions Accepted Manuscript

The UV photo-induced dynamics of thymine and its derivatives involve sub-picosecond relaxation from the $^1\pi\pi^*$ state to the S_0 state in water,[16, 17, 20, 40, 41, 43] acetonitrile[42] and chloroform. Fluorescence up-conversion studies by Gustavsson *et al*. implied that there is some degree of solvent dependence on the direct $^1\pi\pi^* \rightarrow S_0$ process, being (on average) faster in acetonitrile (235 fs) than in water (388 fs).[42] A sub-200 fs decay component was also reported in fluorescence up-conversion experiments on aqueous thymine, dT and dTMP and assigned to relaxation of the $^1\pi\pi^*$ state.[41] This faster $^1\pi\pi^*$ loss could reflect a more direct route to the ethylenic-twist conical intersection with the S_0 ground state,[50] but may also be associated with wavepacket motion out of the fluorescence observation window. Kwok *et al*. observed similarly fast processes by both time-resolved fluorescence and TEAS of an aqueous solution of dT (with $\tau \sim 150$ fs and 760 fs components) and instead argued for sub-ps ISC to the T_1 state.[43] In their time-resolved photoelectron spectroscopy studies of 267-nm excited gas-phase thymine, Ullrich *et al*. reported unassigned time constants of 490 fs and 6.4 ps that bear some resemblance to the solution-phase results, but also observed a <50 fs decay that has not been resolved in solution.[80] Qualitatively similar dynamics were found for the isolated dT nucleoside.[22] A later study by Hudock *et al*.[45] revisited the analysis of the isolated thymine data with the aid of dynamical calculations, and suggested that the sub-500 fs time constants correspond to wavepacket evolution to a local minimum of the $^1\pi\pi^*$ state, rather than any internal conversion process. Meanwhile, the longer picosecond component likely reflects population in the $^1n\pi^*$ state. Other dynamics calculations present a conflicting picture of $^1\pi\pi^* \rightarrow S_0$ internal conversion through an ethylenic-twist conical intersection within ~200 fs,[37] and competing $^1\pi\pi^* \rightarrow {}^1n\pi^*$ internal conversion within ~50 fs.[37, 52] Time-resolved ionization experiments on photoexcited gaseous thymine by Gonzalez et al.[82] observed transient intermediates with lifetimes of <100 fs, 7 ps and >200 ps, with the two longer timescale components either much weaker or missing in clusters of thymine with one or two water molecules. These observations are consistent with sub-ps relaxation on the $^1\pi\pi^*$ state, and longer-time dynamics corresponding to relaxation and then decay of the $^1n\pi^*$ state or involvement of a triplet state. The suppression of these latter channels by water clustering may signal destabilization of the $^1n\pi^*$ state by (even a few) protic solvent molecules.

Faraday Discussions Accepted Manuscript

Once populated from the $^1\pi\pi^*$ state, the $^1n\pi^*$ state of thymine and its derivatives is comparatively long lived,[17] but (as with dC) the lifetime of this excited state is notably sensitive to both solvent and the derivatization at the N1 site. The lifetime variation reflects modifications of the $^1n\pi^*$ potential energy surface and the energy barrier to the conical intersection with the S_0 state. Unlike cytosine derivatives, the quantum yield for ISC to the T_1 ($^3\pi\pi^*$) state is notably enhanced in a number of solvents, and its population is mediated by a vibrationally hot $^1n\pi^*$ state.[17] The growth of T_1 ($^3\pi\pi^*$) absorption bands occurs on comparable (≤10 ps) timescales in both acetonitrile-d_3 and chloroform.[11] A similar timescale emerges from ISC calculations by Etinski *et al*. on isolated thymine.[49] The ISC quantum yields differ by a factor of ~2 in these two solvents, but are an order of magnitude higher than for thymine derivatives in aqueous solution,[11] an effect attributed to destabilization of the intermediate $^1n\pi^*$ state by water solvation.[83]

As was recently summarized by Improta *et al*.,[6] a more qualitatively consistent picture of the relaxation dynamics in thymine derivatives emerges from the recent literature than for cytosine and its derivatives. While there is a degree of quantitative discrepancy, in general, $^1\pi\pi^* \rightarrow S_0$ relaxation is found to occur on a sub-ps timeframe *via* a dominant ethylenic-twist conical intersection. In competition with this direct relaxation, ultrafast $^1\pi\pi^* \rightarrow {}^1n\pi^*$ internal conversion populates a vibrationally hot $^1n\pi^*$ state, which can then either undergo slower relaxation to the S_0 ground state over many picoseconds or act as a doorway for ISC to a long-lived T_1 ($^3\pi\pi^*$) state. Once vibrational cooling has occurred on the $^1n\pi^*$ surface, the ISC channel closes. Consultation of the broad literature shows that the relative importance of these three main relaxation pathways in thymine derivatives depends on the solvation environment.

4. Conclusions

Ultraviolet (λ = 260 nm) absorption by silyl-protected 2'-deoxy-cytidine and 2'-deoxy-thymidine in chloroform solutions initiates ultrafast non-adiabatic dynamics on the photoexcited $^1\pi\pi^*$ state, and on the $^1n\pi^*$ states lying close in energy. These

Faraday Discussions Accepted Manuscript

dynamics are revealed by a combination of ultrafast transient electronic and vibrational absorption spectroscopies. Nuclear motion on the excited states encounters conical intersections with the ground electronic state, and in the case of the amino-oxo canonical form of dC, recovery of the ground state population is essentially complete within 100 ps. Similarly fast repopulation of the ground state occurs in dT, but ~8% of the photoexcited molecules are instead trapped in a long-lived triplet state. The pathways for these various processes involve prompt bifurcation between the $^1\pi\pi^*$ and $^1n\pi^*$ states in the vertical Franck-Condon region, rapid ($\lesssim$ 1 ps) $^1\pi\pi^* \rightarrow S_0$ internal conversion through a conical intersection with ethylenic-twist character, and slower $^1n\pi^* \rightarrow S_0$ internal conversion. The general features of these dynamics appear to be common to both the chosen pyrimidine bases, as well as their nucleosides and nucleotides, but the details of time constants and branching between pathways are sensitive to the functionality at the N1 site of the pyrimidine ring and the properties of the surrounding environment. Recovery of thermalized molecules in their electronic ground state via the $^1n\pi^*$ state takes 18.6 ± 1.1 ps in the amino-oxo form of dC in chloroform, ~114 ps in dT, and 193 ± 55 ps in the minor imino-oxo form of dC. These timescales are mostly controlled by the excited state lifetimes because vibrational cooling of hot ground state molecules requires ~6 ps. A region of singlet-triplet coupling encourages intersystem crossing from the $^1n\pi^*$ state of dT to the T_1 ($^3\pi\pi^*$) state. The $^1n\pi^*$ state lifetime of amino-oxo dC in chloroform is distinctly shorter than those previously reported in methanol and aqueous solutions, indicating either a lower energy $^1n\pi^*/ S_0$ conical intersection in this more weakly interacting solvent, or promotion of AO $^1n\pi^* \rightarrow$ IO $^1n\pi^*$ tautomerization by the protic solvents.

The above interpretation of the dynamics revealed by our TEAS and TVAS measurements is qualitatively in agreement with some, but not all computational studies of the non-adiabatic dynamics of UV-excited cytosine and thymine nucleobases and their derivatives. The outcomes of these computational simulations are highly sensitive to the level of electronic structure theory employed, because of the close proximities of several electronically excited states and the variations in predicted locations of conical intersections which govern the non-adiabatic pathways. Moreover, the dynamics simulations concentrate on processes no longer than a few

Faraday Discussions Accepted Manuscript

picoseconds because of the computational expense of propagating the nuclear dynamics over longer timescales relevant to the $^1n\pi^*$ and triplet state pathways. Conversely, the theoretical simulations predict some <100 fs non-adiabatic dynamics that cannot be distinguished with our current experimental time resolution. We find no evidence to support computational predictions of triplet state formation in photo-excited dC, or bifurcation at the $^1\pi\pi^*/ S_0$ conical intersection which has been proposed as a mechanism for AO $\rightarrow$ IO photo-isomerization.

Unravelling the precise photochemical mechanisms of the monomeric cytosine and thymine nucleobases, and their nucleosides and nucleotides, continues to present a challenge to both experiment and theory. This challenge is still greater when these species are incorporated into Watson-Crick base pairs or nucleic acid strands, where the electronic character of the photoexcitation and the available dynamical and chemical pathways are affected by spatial proximity to other purine or pyrimidine bases.

Acknowledgements

The Bristol group gratefully acknowledges funding from the ERC Advanced Grant 290966 CAPRI. GMR thanks the Ramsay Memorial Trust for the award of a Fellowship. The Kiel group thanks the German Science Foundation (DFG) for financial support through grant SFB 677 and KR acknowledges the DFG for the award of a Research Fellowship. We are grateful to A. S. Henderson, and M. C. Galan (University of Bristol) for help with the synthesis of the derivatized nucleosides, and to M. P. Grubb and P. M. Coulter for assistance with the Bristol transient absorption spectroscopy measurements.

All experimental data are archived in the University of Bristol's Research Data Storage Facility (DOI: 10.5523/bris.re6ei611x5in1quskmq7dft3m).

Faraday Discussions Accepted Manuscript

Figure 1

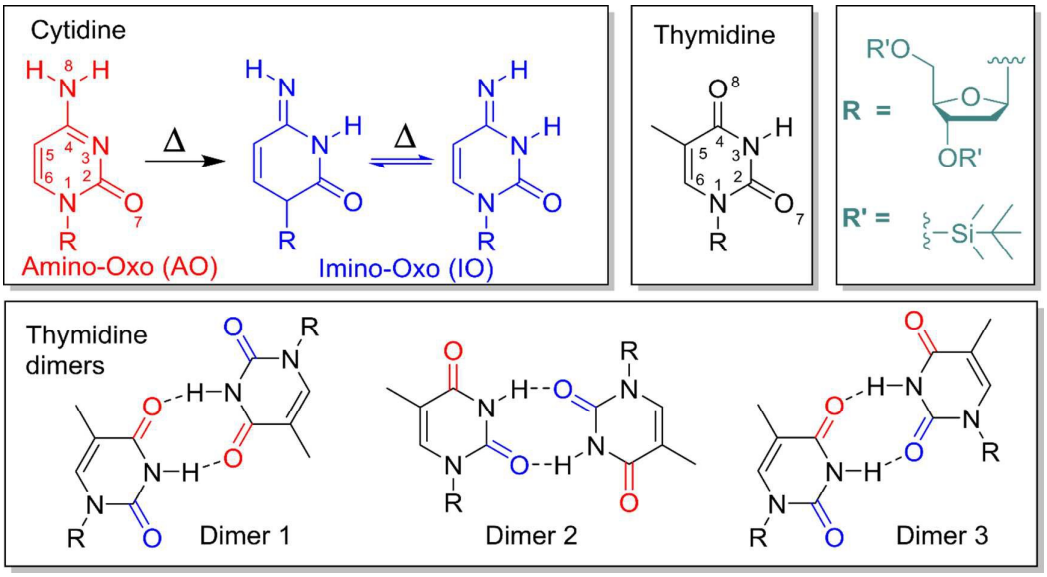

Fig. 1. Molecular structures of the amino-oxo (AO, red) and imino-oxo (IO, blue) tautomers of the protected cytidine (dC) and protected thymidine (dT, black) nucleosides. Possible hydrogen-bonded dT•dT dimer structures and the structures of the silyl protected 2'-deoxy-ribose groups (grey) are also shown. The scheme for dC shows thermally induced tautomerization between AO and IO.

Faraday Discussions Accepted Manuscript

Figure 2

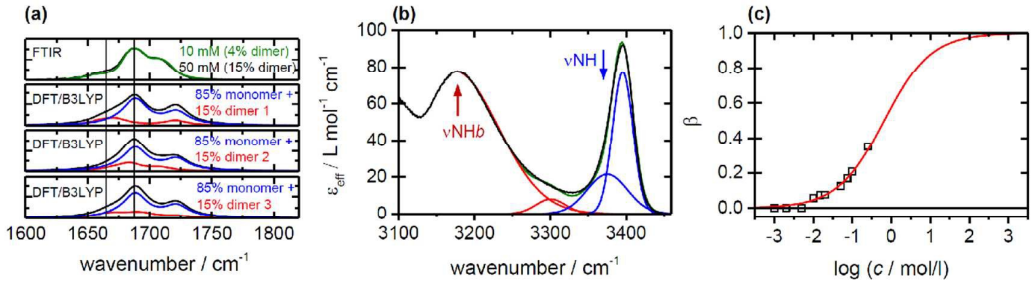

Fig. 2. (a) Top panel: Concentration dependent FTIR spectra of dT solutions in $CHCl_3$ recorded at c_0 = 10 mM (green) and c_0 = 50 mM (black) in the carbonyl stretch region. dT•dT dimer fractions are also shown. Lower panels: Simulated FTIR spectra of 50 mM dT solutions in chloroform, calculated at the PCM-B3LYP/6-311++G** level of theory. Calculated harmonic vibrational frequencies are scaled by 0.993 for monomers and dimers. The three simulated spectra (black) are constructed assuming an 85% dT monomer contribution (blue) together with a 15% dT•dT fraction (red) from either dimer 1, dimer 2 or dimer 3 (see Fig. 1). (b) Example FTIR spectrum for a 50 mM dT solution in $CHCl_3$ in the N-H stretching region (black) together with a fit (green) consisting of monomer (νNH, blue) and dimer (νNH*b*, red) contributions. (c) Degree of association (β_{TT}) obtained from the concentration dependent FTIR band fitting analysis in the N-H stretching region (b) for dT•dT dimerization in $CHCl_3$ as a function of $\log(c_0)$.

Faraday Discussions Accepted Manuscript

Figure 3

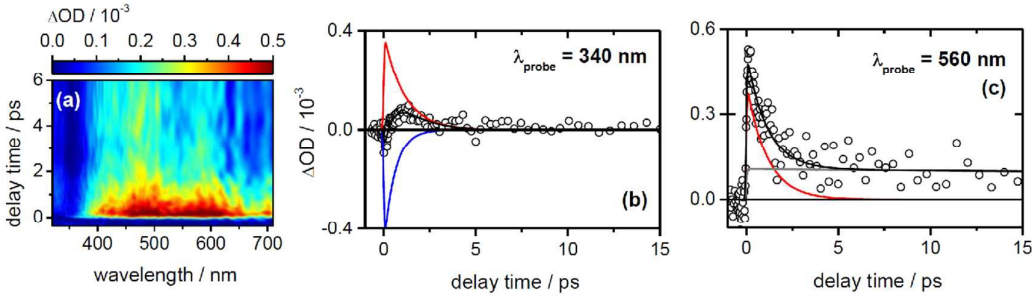

Fig. 3. (a) Two-dimensional false colour intensity map of the TEA spectrum obtained from C (c_0 = 10 mM) in $CHCl_3$ following excitation at 260 nm (C = 65%, C•C = 35%). Absorption change profiles as a function of delay time obtained from (a) at probe wavelengths of (b) λ_{probe} = 340 nm and (c) λ_{probe} = 560 nm. Open circles = experimental data, black line = total fit. Coloured lines are decay components with time constants of τ_1 = 0.6 ps (blue line), τ_2 = 1.1 ps (red line) and τ_3 = 193 ps (grey line). See Table 2 for details of τ_n fit amplitudes (A_n).

Faraday Discussions Accepted Manuscript

Figure 4

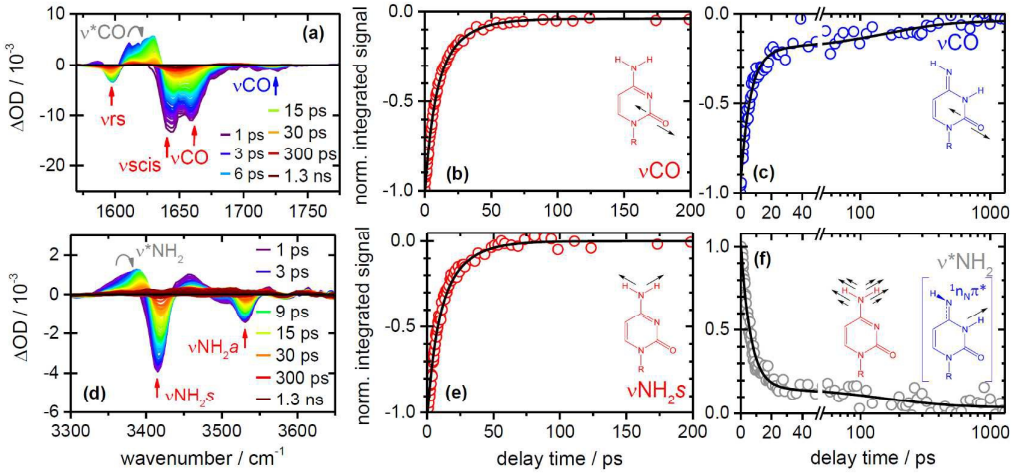

Fig. 4. TVA spectra recorded for dC (c_0 = 5 mM) in $CDCl_3$ following excitation at 260 nm and probing in (a) the carbonyl stretch region (1550 - 1775 cm^{-1}) and (b) the NH_2 stretching region (3300 - 3650 cm^{-1}) (dC = 76%, dC•dC = 24%). Normalized integrated signal traces (open circles) and kinetic fits (black lines) as a function of delay time for (b) the carbonyl bleach (νCO, 1660 cm^{-1}) of the AO tautomer, (c) the carbonyl bleach (νCO, 1720 cm^{-1}) of the IO tautomer, (e) the symmetric NH_2 stretch bleach ($\nu NH_2 s$, 3410 cm^{-1}) of the AO tautomer, and (f) vibrationally hot NH_2 ground state (ν∗NH_2, 3380 cm^{-1}). ν∗NH_2 also contains contributions from the $^1n_N\pi^*$ state of the IO tautomer – see main text for details. See Table 2 for details of τ_n fit amplitudes (A_n).

Faraday Discussions Accepted Manuscript

Figure 5

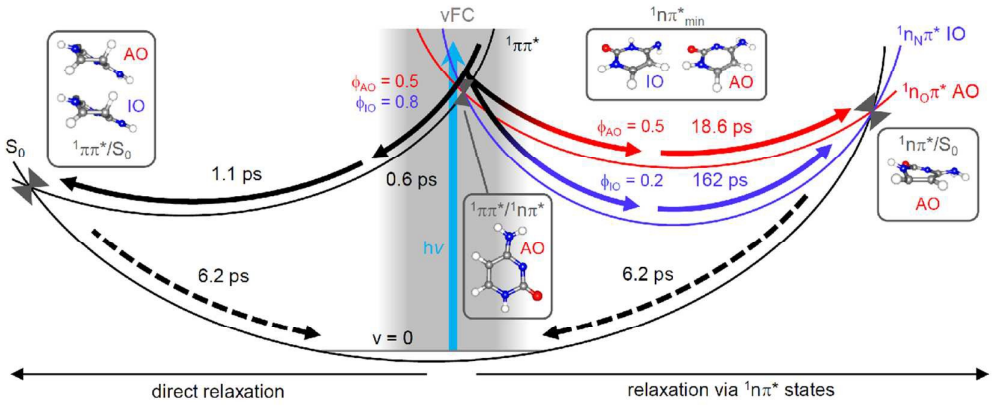

Fig. 5. Schematic potential energy cuts through the S_0, $^1\pi\pi^*$, $^1n_O\pi^*$ and $^1n_N\pi^*$ electronic states for the AO and IO tautomers of dC, depicting a plausible kinetic scheme for the excited state relaxation of dC in chloroform based on TVAS and TEAS measurements with 260 nm excitation. Black = IO and AO, Red = AO only, Blue = IO only. Possible structures involved in the relaxation dynamics are obtained from theoretical calculations on the AO and IO tautomers of the simpler cytosine nucleobase in the gas-phase; $^1\pi\pi^*/S_0$ AO and $^1\pi\pi^*/^1n\pi^*$ AO from Ref. 37, $^1n\pi^*/S_0$ AO and $^1n\pi^*_{min}$ AO from Ref. 38, $^1\pi\pi^*/S_0$ IO and $^1n\pi^*_{min}$ IO from Ref. 27. The values of ϕ denote branching between competing channels.

Faraday Discussions Accepted Manuscript

Figure 6

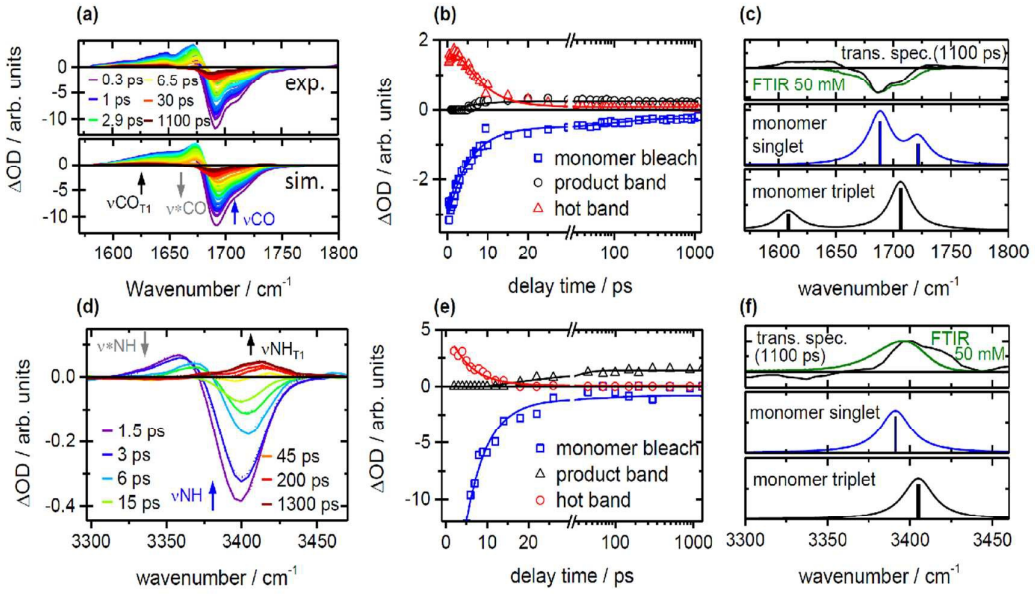

Fig. 6. TVA spectra recorded for dT (c_0 = 50 mM) in $CHCl_3$ following excitation at 260 nm and probing in (a) the carbonyl stretch region (1550 - 1800 cm^{-1}) and (d) the N-H stretching region (3300 - 3475 cm^{-1}) (dT = 85%, dT•dT = 15%). Experimental (upper panel) and simulated fitted spectra (lower panel) are shown in (a), while in (d) solid and dashed lines represent experiment and fits, respectively. Integrated fitted band signals (symbols) and kinetic fits (solid lines) as a function of delay time for: (b) the carbonyl bleach (νCO, blue), the vibrationally hot CO ground state (ν*CO, red) and T_1 triplet state product band (νCO_{T1}, black); and (e) the NH stretch bleach (νNH, blue), the vibrationally hot N-H stretch ground state (ν*NH, red) and T_1 triplet state product band (νNH_{T1}, black). (c) and (f) compare (upper panels) TVA spectra recorded at t = 1.1 ns (black) and FTIR spectra (green), together with (middle panels) calculated vibrational spectra for the S_0 ground state of the dT monomer and (lower panels) T_1 ($^3\pi\pi^*$) state of the dT monomer at the PCM-B3LYP/6-311++G** level of theory. Calculated harmonic vibrational frequencies are scaled by 0.993 in the carbonyl stretching region and 0.945 in the N-H stretching region.

Faraday Discussions Accepted Manuscript

Figure 7

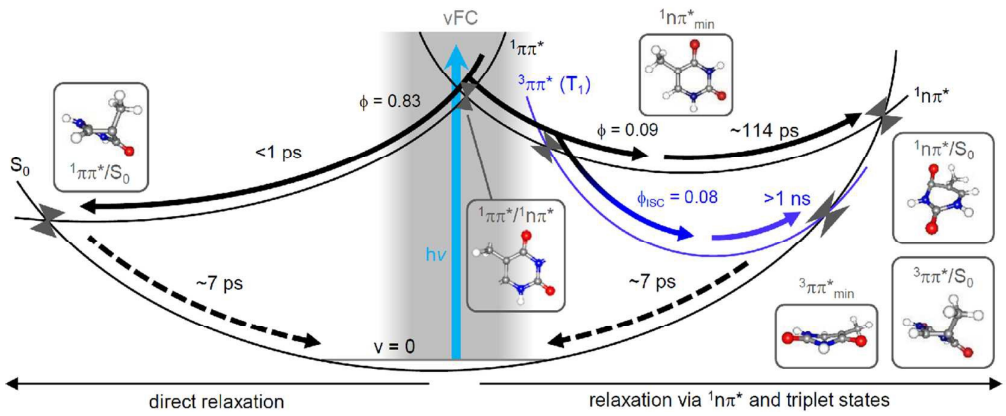

Fig. 7. Schematic potential energy cuts through the S_0, $^1\pi\pi^*$, $^1n\pi^*$ and $^3\pi\pi^*$ electronic states of dT, depicting a plausible kinetic scheme for the excited state relaxation of dT in chloroform based on TVAS measurements at 260 nm. Black = singlet states, blue = triplet states. Possible structures involved in the relaxation dynamics are obtained from theoretical calculations on the simpler thymine nucleobase in the gas-phase; $^1\pi\pi^*/S_0$, $^1\pi\pi^*/^1n\pi^*$, $^1n\pi^*_{min}$ and $^1n\pi^*/S_0$ from Ref. 37, $^3\pi\pi^*/S_0$ and $^3\pi\pi^*_{min}$ from Ref. 46. The values of ϕ denote branching between competing channels.

Faraday Discussions Accepted Manuscript

Table 1. Degrees of association (β) into dC•dC or dT•dT dimers for different concentrations of cytidine and thymidine in chloroform.

c_0 / mM	β_{CC}	β_{TT}
5	0.24	0.02
10	0.35	0.04
25	0.51	0.09
50	0.62	0.15

Table 2. Extracted time constant values (τ_n), their respective fit amplitudes (A_n) and photophysical assignments, from a global fitting analysis of the kinetic traces obtained from TEAS (Fig. 3) and TVAS (Fig. 4) measurements on dC in chloroform at 260 nm.

[a] A modified value of $\tau_3' = 162 \pm 48$ ps is required to fit the TVAS data.

		TEAS		TVAS				
Time Constant (τ_n)	Value / ps	A_n (λ_{pr} = 340 nm)	A_n (λ_{pr} = 560 nm)	A_n (νCO_{AO})	A_n (νCO_{IO})	A_n ($\nu NH_2 s$)	A_n ($\nu^* NH_2$)	Assignment
τ_1	0.6 ± 0.5	-0.55	-	-	-	-	-	vFC SE
τ_2	1.1 ± 0.1	0.45	0.80	-	-	-	-	$^1\pi\pi^*$ decay
τ_3	193 ± 55[a]	-	0.20	-	0.17	-	0.12	$^1n_N\pi^*$ IO decay
τ_4	6.2 ± 0.3	-	-	0.49	0.78	0.44	0.85	S_0 vib. cooling
τ_5	18.6 ± 1.1	-	-	0.48	-	0.56	-	$^1n_O\pi^*$ AO decay
τ_6	∞	-	-	0.03	0.05	-	0.03	dC•dC dimer

Table 3. Extracted time constant values (τ_n), their respective fit amplitudes (A_n) and photophysical assignments, from a global fitting analysis of the kinetic traces obtained from TVAS (Fig. 6) measurements on dT in chloroform at 260 nm excitation.

[a] Averaged value for the N-H stretch and carbonyl regions.

[b] The rise time of ν*NH is < 1 ps and masked by experimental complications and/or our time resolution.

Time Constant (τ_n)	Value / ps	A_n (νCO)	A_n ($\nu^* CO$)	A_n (νCO_{T1})	A_n (νNH)	A_n ($\nu^* NH$)	A_n (νNH_{T1})	Assignment
τ_1	7 ± 2 [a]	0.83	decay time	rise time	0.96	decay time	rise time	v=1 → v=0 vib. cooling
τ_2	~114	0.09	-	-	0.01	-	-	$^1n\pi^*$ decay

Faraday Discussions Accepted Manuscript

τ_3	∞	0.08	-	decay time	0.03	-	decay time	$^3\pi\pi^*$ decay
τ_4	2.4 ± 0.6^b	-	rise time	-	-	[b]	-	v>1 → v=1 S_0 vib. cooling
τ_5	5-10	-	-	onset	-	-	onset	$^1n\pi^* \rightarrow {}^3\pi\pi^*$ ISC

Table 4. Comparison of dynamical process time constants and intersystem crossing quantum yields (ϕ_{ISC}) obtained for the photodynamics of cytosine and thymine derivatives in different solvents following excitation at wavelengths between 260 and 270 nm (unless stated otherwise). C = cytidine, CMP = cytidine 5'-monophosphate, T = thymidine, TMP = thymidine 5'-monophosphate, d = 2'-deoxy-ribose form.

[a] $^1n_N\pi^*$ state lifetime obtained for the minor imino-oxo tautomer.

[b] Hare *et al*. stated equal $^1n\pi^*$ lifetimes for dT and dTMP.

[c] Values are for the amino-oxo form in the gas-phase

[d] Recorded in acetonitrile-d_3

[e] Obtained from TEAS on C.

	Dynamical Process Time Constant / ps				
Derivative & Solvent	$^1\pi\pi^* \rightarrow S_0$	$^1n\pi^* \rightarrow S_0$	$^1n\pi^* \rightarrow T_1$	ϕ_{ISC} (T_1)	References
Cytosine in water	0.7	12	-	≤0.04	17
Cytosine in methanol	1.1	52	-	-	21
CMP in water	0.7	34	-	≤0.07	17
dCMP in water	1.3	33	-	-	18, 21
C in water	1.8	35	-	-	21
C in methanol	1.3	144	-	-	21
dC in water	0.7	37	-	-	18, 21, 33
dC in methanol	0.8	186	-	-	21
dC in chloroform	1.1[e]	18 (193 [a])	-	-	this work
Cytosine in gas-phase [c]					
λ_{exc} > 310 nm	30-730	-	-	<0.05	39, 73, 81
λ_{exc} = 290 nm	1.1	(≥150 [a])	-	-	67
C in gas-phase	0.74	-	-	-	22
Thymine in water	0.72	30	-	≤0.02	17
Thymine in acetonitrile	<1.1	-	≤10[d]	~0.2 [d]	11, 42
dTMP in water	0.41	127	-	≤0.013	17
dT in water	0.54	127 [b]	-	-	15-17
dT in acetonitrile	-	-	≤10[d]	~0.2 [d]	11
dT in chloroform	<1	~114	5-10	0.08	this work
Thymine in gas-phase	0.46	6.4	-	-	36, 80

Faraday Discussions Accepted Manuscript

dT in gas-phase	2.9	-	-	-	22

References

1. C. E. Crespo-Hernandez, B. Cohen, P. M. Hare and B. Kohler, *Chem. Rev.*, 2004, **104**, 1977-2019.
2. C. T. Middleton, K. de La Harpe, C. Su, Y. K. Law, C. E. Crespo-Hernandez and B. Kohler, *Annu Rev Phys Chem*, 2009, **60**, 217-239.
3. A. H. Zewail, *J. Phys. Chem. A*, 2000, **104**, 5660-5694.
4. W. Domcke, D. R. Yarkony and H. Koppel, eds., *Conical Intersections: Theory, Computation and Experiment*, World Scientific, 2011.
5. M. Barbatti, A. J. A. Aquino, J. J. Szymczak, D. Nachtigallova, P. Hobza and H. Lischka, *P Natl Acad Sci USA*, 2010, **107**, 21453-21458.
6. R. Improta, F. Santoro and L. Blancafort, *Chem. Rev.*, 2016, DOI: 10.1021/acs.chemrev.1025b00444.
7. Z. Y. Liu, C. Tan, X. M. Guo, Y. T. Kao, J. Li, L. J. Wang, A. Sancar and D. P. Zhong, *Proc. Natl. Acad. Sci. U. S. A.*, 2011, **108**, 14831-14836.
8. J. Li, Z. Y. Liu, C. Tan, X. M. Guo, L. J. Wang, A. Sancar and D. P. Zhong, *Nature*, 2010, **466**, 887.
9. Z. Y. Liu, L. J. Wang and D. P. Zhong, *Phys. Chem. Chem. Phys.*, 2015, **17**, 11933-11949.
10. D. W. Whillans and H. E. Johns, *J. Am. Chem. Soc.*, 1971, **93**, 1358.
11. P. M. Hare, C. T. Middleton, K. I. Mertel, J. M. Herbert and B. Kohler, *Chem. Phys.*, 2008, **347**, 383-392.
12. A. A. Lamola and J. P. Mittal, *Science*, 1966, **154**, 1560.
13. W. J. Schreier, T. E. Schrader, F. O. Koller, P. Gilch, C. E. Crespo-Hernandez, V. N. Swaminathan, T. Carell, W. Zinth and B. Kohler, *Science*, 2007, **315**, 625-629.
14. K. Siriwong, A. A. Voityuk, M. D. Newton and N. Rosch, *J. Phys. Chem. B*, 2003, **107**, 2595-2601.

Faraday Discussions Accepted Manuscript

15. J. M. L. Pecourt, J. Peon and B. Kohler, *J Am Chem Soc*, 2000, **122**, 9348-9349.
16. J. M. L. Pecourt, J. Peon and B. Kohler, *J Am Chem Soc*, 2001, **123**, 10370-10378.
17. P. M. Hare, C. E. Crespo-Hernandez and B. Kohler, *Proc. Natl. Acad. Sci. U. S. A.*, 2007, **104**, 435-440.
18. S. Quinn, G. W. Doorley, G. W. Watson, A. J. Cowan, M. W. George, A. W. Parker, K. L. Ronayne, M. Towrie and J. M. Kelly, *Chem. Commun.*, 2007, 2130-2132.
19. N. K. Schwalb, T. Michalak and F. Temps, *J Phys Chem B*, 2009, **113**, 16365-16376.
20. J. Peon and A. H. Zewail, *Chem Phys Lett*, 2001, **348**, 255-262.
21. C. S. Ma, C. C. W. Cheng, C. T. L. Chan, R. C. T. Chan and W. M. Kwok, *Phys. Chem. Chem. Phys.*, 2015, **17**, 19045-19057.
22. S. De Camillis, J. Miles, G. Alexander, O. Ghafur, I. D. Williams, D. Townsend and J. B. Greenwood, *Phys. Chem. Chem. Phys.*, 2015, **17**, 23643-23650.
23. N. Ismail, L. Blancafort, M. Olivucci, B. Kohler and M. A. Robb, *J. Am. Chem. Soc.*, 2002, **124**, 6818-6819.
24. M. Merchan and L. Serrano-Andres, *J. Am. Chem. Soc.*, 2003, **125**, 8108-8109.
25. L. Blancafort and M. A. Robb, *J. Phys. Chem. A*, 2004, **108**, 10609-10614.
26. M. Merchan, L. Serrano-Andres, M. A. Robb and L. Blancafort, *J. Am. Chem. Soc.*, 2005, **127**, 1820-1825.
27. K. Tomic, J. Tatchen and C. M. Marian, *J. Phys. Chem. A*, 2005, **109**, 8410-8418.
28. M. Merchan, R. Gonzalez-Luque, T. Climent, L. Serrano-Andres, E. Rodriuguez, M. Reguero and D. Pelaez, *J. Phys. Chem. B*, 2006, **110**, 26471-26476.
29. L. Blancafort, *Photochem. Photobiol.*, 2007, **83**, 603-610.
30. K. A. Kistler and S. Matsika, *J. Phys. Chem. A*, 2007, **111**, 2650-2661.
31. J. Gonzalez-Vazquez and L. Gonzalez, *ChemPhysChem*, 2010, **11**, 3617-3624.
32. Q. S. Li and L. Blancafort, *Photochem. Photobiol. Sci.*, 2013, **12**, 1401-1408.

Faraday Discussions Accepted Manuscript

33. C. G. Triandafillou and S. Matsika, *J. Phys. Chem. A*, 2013, **117**, 12165-12174.
34. M. Richter, P. Marquetand, J. Gonzalez-Vazquez, I. Sola and L. Gonzalez, *J. Phys. Chem. Lett.*, 2012, **3**, 3090-3095.
35. S. Mai, P. Marquetand, M. Richter, J. Gonzalez-Vazquez and L. Gonzalez, *ChemPhysChem*, 2013, **14**, 2920-2931.
36. H. R. Hudock and T. J. Martinez, *ChemPhysChem*, 2008, **9**, 2486-2490.
37. Z. G. Lan, E. Fabiano and W. Thiel, *J Phys Chem B*, 2009, **113**, 3548-3555.
38. M. Barbatti, A. J. A. Aquino, J. J. Szymczak, D. Nachtigallova and H. Lischka, *Phys. Chem. Chem. Phys.*, 2011, **13**, 6145-6155.
39. S. Blaser, M. A. Trachsel, S. Lobsiger, T. Wiedmer, H. Frey and S. Leutwyler, *J. Phys. Chem. Lett.*, 2016, **7**, 752-757.
40. F. Buchner, A. Nakayama, S. Yamazaki, H. H. Ritze and A. Lubcke, *J. Am. Chem. Soc.*, 2015, **137**, 2931-2938.
41. T. Gustavsson, A. Sharonov and D. Markovitsi, *Chem. Phys. Lett.*, 2002, **351**, 195-200.
42. T. Gustavsson, N. Sarkar, E. Lazzarotto, D. Markovitsi and R. Improta, *Chem. Phys. Lett.*, 2006, **429**, 551-557.
43. W. M. Kwok, C. Ma and D. L. Phillips, *J. Am. Chem. Soc.*, 2008, **130**, 5131-5139.
44. S. Perun, A. L. Sobolewski and W. Domcke, *J. Phys. Chem. A*, 2006, **110**, 13238-13244.
45. H. R. Hudock, B. G. Levine, A. L. Thompson, H. Satzger, D. Townsend, N. Gador, S. Ullrich, A. Stolow and T. J. Martinez, *J. Phys. Chem. A*, 2007, **111**, 8500-8508.
46. J. J. Serrano-Perez, R. Gonzalez-Luque, M. Merchan and L. Serrano-Andres, *J. Phys. Chem. B*, 2007, **111**, 11880-11883.
47. G. Zechmann and M. Barbatti, *J. Phys. Chem. A*, 2008, **112**, 8273-8279.
48. J. J. Szymczak, M. Barbatti, J. T. S. Hoo, J. A. Adkins, T. L. Windus, D. Nachtigallova and H. Lischka, *J. Phys. Chem. A*, 2009, **113**, 12686-12693.
49. M. Etinski, T. Fleig and C. A. Marian, *J. Phys. Chem. A*, 2009, **113**, 11809-11816.
50. D. Asturiol, B. Lasorne, M. A. Robb and L. Blancafort, *J. Phys. Chem. A*, 2009, **113**, 10211-10218.

Faraday Discussions Accepted Manuscript

51. R. Gonzalez-Luque, T. Climent, I. Gonzalez-Ramirez, M. Merchan and L. Serrano-Andres, *J. Chem. Theory Comput.*, 2010, **6**, 2103-2114.
52. D. Picconi, V. Barone, A. Lami, F. Santoro and R. Improta, *ChemPhysChem*, 2011, **12**, 1957-1968.
53. C. Salet, R. Bensasson and R. S. Becker, *Photochem. Photobiol.*, 1979, **30**, 325-329.
54. H. Gorner, *J. Photochem. Photobiol. B*, 1990, **5**, 359-377.
55. T. Climent, I. Gonzalez-Ramirez, R. Gonzalez-Luque, M. Merchan and L. Serrano-Andres, *J Phys Chem Lett*, 2010, **1**, 2072-2076.
56. M. M. Brister and C. E. Crespo-Hernandez, *J Phys Chem Lett*, 2015, **6**, 4404-4409.
57. H. E. Johns, M. Delbruck and S. A. Rapaport, *J Mol Biol*, 1962, **4**, 104.
58. H. E. Johns, M. L. Pearson, C. W. Helleiner and J. C. Leblanc, *J Mol Biol*, 1964, **9**, 503-&.
59. C. F. Yang, Y. Q. Yu, K. H. Liu, D. Song, L. D. Wu and H. M. Su, *Journal of Physical Chemistry A*, 2011, **115**, 5335-5345.
60. M. C. Cuquerella, V. Lhiaubet-Vallet, F. Bosca and M. A. Miranda, *Chem Sci*, 2011, **2**, 1219-1232.
61. K. K. Ogilvie, *Can. J. Chem.*, 1973, **51**, 3799-3807.
62. K. Rottger, H. J. B. Marroux, M. P. Grubb, P. M. Coulter, H. Bohnke, A. S. Henderson, M. C. Galan, F. Temps, A. J. Orr-Ewing and G. M. Roberts, *Angewandte Chem. Int. Ed.*, 2015, **54**, 14719-14722.
63. K. Rottger, R. Siewertsen and F. Temps, *Chem. Phys. Lett.*, 2012, **536**, 140-146.
64. K. Rottger, S. Wang, F. Renth, J. Bahrenburg and F. Temps, *Appl. Phys. B*, 2015, **118**, 185-193.
65. L. Biemann, S. A. Kovalenko, K. Kleinermanns, R. Mahrwald, M. Markert and R. Improta, *J. Am. Chem. Soc.*, 2011, **133**, 19664-19667.
66. G. M. Roberts, H. J. B. Marroux, M. P. Grubb, M. N. R. Ashfold and A. J. Orr-Ewing, *J. Phys. Chem. A*, 2014, **118**, 11211-11225.
67. K. Kosma, C. Schroter, E. Samoylova, I. V. Hertel and T. Schultz, *J. Am. Chem. Soc.*, 2009, **131**, 16939-16943.
68. L. Buschhaus, J. Rolf and K. Kleinermanns, *Phys. Chem. Chem. Phys.*, 2013, **15**, 18371-18377.

Faraday Discussions Accepted Manuscript

69. I. Reva, M. J. Nowak, L. Lapinski and R. Fausto, *J. Phys. Chem. B*, 2012, **116**, 5703-5710.

70. M. J. Frisch, G. W. Trucks, H. B. Schlegel, G. E. Scuseria, M. A. Robb, J. R. Cheeseman, G. Scalmani, V. Barone, B. Mennucci, G. A. Petersson, H. Nakatsuji, M. Caricato, X. Li, H. P. Hratchian, A. F. Izmaylov, J. Bloino, G. Zheng, J. L. Sonnenberg, M. Hada, M. Ehara, K. Toyota, R. Fukuda, J. Hasegawa, M. Ishida, T. Nakajima, Y. Honda, O. Kitao, H. Nakai, T. Vreven, J. A. Montgomery, J. E. Peralta, F. Ogliaro, M. J. Bearpark, J. J. Heyd, E. Brothers, K. N. Kudin, V. N. Staroverov, R. Kobayashi, J. Normand, K. Raghavachari, A. Rendell, J. C. Burant, S. S. Iyengar, J. Tomasi, M. Cossi, N. Rega, J. M. Millam, M. Klene, J. E. Knox, J. B. Cross, V. Bakken, C. Adamo, J. Jaramillo, R. Gomperts, R. E. Stratmann, O. Yazyev, A. J. Austin, R. Cammi, C. Pomelli, J. W. Ochterski, R. L. Martin, K. Morokuma, V. G. Zakrzewski, G. A. Voth, P. Salvador, J. J. Dannenberg, S. Dapprich, A. D. Daniels, O. Farkas, J. B. Foresman, J. V. Ortiz, J. Cioslowski and D. J. Fox, *Gaussian 09; Gaussian Inc.: Wallingford, CT, 2009.*, 2009.

71. D. Murdock, S. J. Harris, J. Luke, M. P. Grubb, A. J. Orr-Ewing and M. N. R. Ashfold, *Phys. Chem. Chem. Phys.*, 2014, **16**, 21271-21279.

72. M. A. El-Sayed, *Acc. Chem. Res.*, 1968, **1**, 8-16.

73. S. Lobsiger, M. A. T'rachsel, H. M. Frey and S. Leutwyler, *J. Phys. Chem. B*, 2013, **117**, 6106-6115.

74. C. Canuel, M. Mons, F. Piuzzi, B. Tardivel, I. Dimicoli and M. Elhanine, *J Chem Phys*, 2005, **122**, 074316.

75. J. W. Ho, H. C. Yen, W. K. Chou, C. N. Weng, L. H. Cheng, H. Q. Shi, S. H. Lai and P. Y. Cheng, *J. Phys. Chem. A*, 2011, **115**, 8406-8418.

76. R. J. Malone, A. M. Miller and B. Kohler, *Photochem. Photobiol.*, 2003, **77**, 158-164.

77. A. Sharonov, T. Gustavsson, V. Carre, E. Renault and D. Markovitsi, *Chem. Phys. Lett.*, 2003, **380**, 173-180.

78. A. Sharonov, T. Gustavsson, S. Marguet and D. Markovitsi, *Photochem. Photobiol. Sci.*, 2003, **2**, 362-364.

79. L. Blancafort, B. Cohen, P. M. Hare, B. Kohler and M. A. Robb, *J Phys Chem A*, 2005, **109**, 4431-4436.

Faraday Discussions Accepted Manuscript

80. S. Ullrich, T. Schultz, M. Z. Zgierski and A. Stolow, *Phys. Chem. Chem. Phys.*, 2004, **6**, 2796-2801.

81. S. Lobsiger, M. Etinski, S. Blaser, H. M. Frey, C. Marian and S. Leutwyler, *J. Chem. Phys.*, 2015, **143**, 234301.

82. J. Gonzalez-Vazquez, L. Gonzalez, E. Samoylova and T. Schultz, *Phys. Chem. Chem. Phys.*, 2009, **11**, 3927-3934.

83. M. Etinski and C. M. Marian, *Phys. Chem. Chem. Phys.*, 2010, **12**, 4915-4923.

Faraday Discussions Accepted Manuscript